

A New Formulation for Characterization of Materials Based on Measured Insertion Transfer Function

Ali Hussein Muqaibel, *Student Member, IEEE*, and Ahmad Safaai-Jazi, *Senior Member, IEEE*,

Abstract—A widely used method for noncontact electromagnetic characterization of materials is based on the measurement of an insertion transfer function. This function, defined as the ratio of two phasor signals measured in the presence and absence of the material under test, is related to the dielectric constant of the material through a complex transcendental equation. Solving this equation requires a numerical two-dimensional root search technique, which is often time consuming due to slow convergence and the existence of spurious solutions. In this paper, a new formulation is presented, which facilitates the evaluation of complex dielectric constant of low-loss materials by means of real equations, thus requiring only one-dimensional root search techniques. Two sample materials are measured, and it is shown that their dielectric constants obtained from the exact complex equation and the new formulation are in excellent agreement. The new formulation reduces the computation time significantly and is highly accurate for the characterization of low-loss materials.

Index Terms—Dielectric materials, dielectric measurements, pulse measurements.

I. INTRODUCTION

ELECTROMAGNETIC characterization of materials is essential to many applications, including design and modeling of transmission lines, microwave devices, and optical components, and more recently, to wave propagation in indoor environments [1]–[3]. Various techniques have been developed for the characterization of materials, each with its unique capabilities and advantages. Here, attention is focused on a characterization method based on the measurement of an *insertion transfer function* using radiated fields [4]. When time-domain radiated measurements are used, a short-duration electromagnetic pulse, $\mathbf{E}_i(t, \mathbf{r})$, is applied to a material layer of thickness d . The materials slab is assumed to be homogeneous, isotropic, and linear. The incident pulse is partially transmitted through the slab and is partially reflected, with multiple reflections occurring between the slab boundaries. The transmitted signal $\mathbf{E}_t(t, \mathbf{r})$ results in a voltage at the receive antenna terminals. By measuring two received signals, one with the slab material in place and another without the slab, and taking the ratio of the Fourier transforms of the two signals, one is able to determine the insertion transfer function of the slab material. The insertion transfer function can

also be measured in the frequency domain using a network analyzer. The complex dielectric constant of the material under test can then be extracted from the measured insertion transfer function [5], [6].

If the duration of the pulse is smaller than the pulse travel time through the slab, a *single-pass* technique can be used to obtain the insertion transfer function. Multiple reflections inside the layer, which are delayed by more than the pulse duration, can be eliminated by means of time gating [7]. A *multipass* technique should be used when multiple reflections inside the slab cannot be separated from the first-pass portion of the transmitted signal. On the other hand, from the analysis of a plane wave normally incident upon a one-dimensional slab material, an expression for the insertion transfer function can be derived. This expression, in addition to the insertion transfer function, includes the complex dielectric constant of the material, slab thickness, and frequency. With the insertion transfer function obtained by measurements and the slab thickness known, the expression is a complex transcendental equation, which can be solved for the complex dielectric constant of the material at a given frequency [8].

Solving a complex equation requires a two-dimensional root search, which is often time consuming. For most materials of interest, losses are small, yet a two-dimensional search has been used for the calculation of dielectric constant. In this paper, a new formulation for the evaluation of complex dielectric constant is presented, which is applicable to materials with relatively small losses. In this formulation, only real equations are solved using one-dimensional root search techniques, which also have the advantage of reducing the processing time and improving the convergence of the search algorithm.

II. MEASUREMENT OF INSERTION TRANSFER FUNCTION

The insertion transfer function is obtained through two measurements, as shown schematically in Fig. 1. The measurements may be performed in either the time domain using short duration pulses, or in the frequency domain using sinusoidal signals. The measurement procedure is as follows. The transmit and receive antennas are kept at fixed locations and aligned for maximum reception. The material to be measured is placed at nearly the midpoint between the two antennas. The distance between the antennas should be sufficiently large such that the material object is in the far field of each antenna. With this arrangement, the electromagnetic field incident on the material is essentially a plane wave. The material is assumed to be in the form of a slab with thickness d and held in position such that the plane wave is normally incident on it, as shown in Fig. 1. After the measurement system is set up, we first measure the time-domain

Manuscript received November 6, 2002; revised February 21, 2003. This work was supported in part by the Defense Advanced Research Projects Agency under the Networking in Extreme Environments Program.

The authors are with the Time-Domain and RF Measurement Laboratory, Bradley Department of Electrical and Computer Engineering, Virginia Polytechnic Institute and State University, Blacksburg, VA 24061-0111 USA (e-mail: ajazi@vt.edu).

Digital Object Identifier 10.1109/TMTT.2003.815274

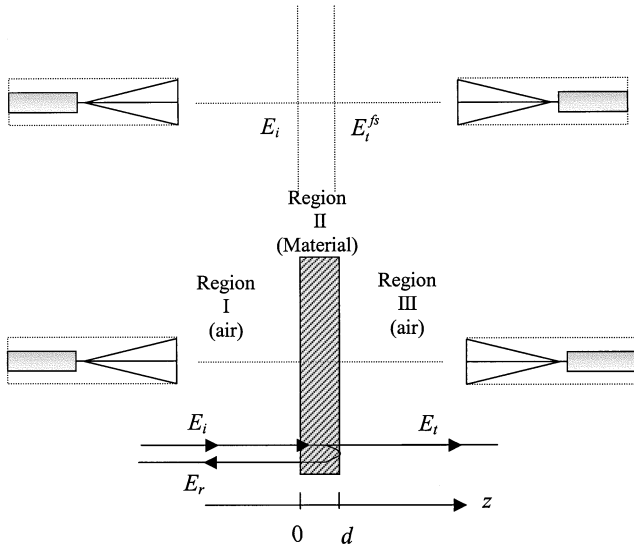


Fig. 1. Propagation through a slab for radiated measurement of an insertion transfer function.

signal $v_t^{fs}(t)$ with a sampling oscilloscope or the frequency-domain signal $V_t^{fs}(j\omega)$ with a network analyzer in the absence of the material. We then measure the time-domain signal $v_t(t)$ or the frequency-domain signal $V_t(j\omega)$ with the material layer in place. The insertion transfer function is then calculated as

$$H(j\omega) \equiv \frac{\frac{E_t(j\omega)}{E_i(j\omega)}}{\frac{E_t^{fs}(j\omega)}{E_i(j\omega)}} = \frac{E_t(j\omega)}{E_t^{fs}(j\omega)} = \frac{\text{FFT}(v_t(t))}{\text{FFT}(v_t^{fs}(t))} = \frac{V_t(j\omega)}{V_t^{fs}(j\omega)} \quad (1)$$

where $\omega = 2\pi f$ is the angular frequency and the fast Fourier transform (FFT) is used to convert the sampled signal to the frequency-domain data. Care must be taken to ensure that the conditions for the free-space measurement are as closely identical as possible to those for the measurement through the material slab.

If single-pass short-pulse propagation measurements can be performed without difficulty and the material can be assumed to be low loss, the dielectric constant and loss tangent can be obtained following the approach presented in [5]. However, if the single-pass signal cannot be gated out satisfactorily, multiple reflections from the slab interior that constitute part of the received signal must be accounted for. This situation particularly arises when the transit time through the slab thickness is small compared to the pulse duration. In this case, an insertion transfer function that accounts for multiple reflections should be used.

III. EVALUATION OF COMPLEX DIELECTRIC CONSTANT

In order to determine the complex dielectric constant from the measured insertion transfer function, an expression for $H(j\omega)$ is needed. To calculate $H(j\omega)$, let us assume that an x -polarized uniform plane-wave, representing the local far field of the transmit antenna, is normally incident on a slab of material with thickness d . The material has an unknown complex dielectric constant $\varepsilon_r = \varepsilon_r' - j\varepsilon_r''$. The incident plane wave, as depicted in Fig. 1, establishes a reflected wave in region I (air), a set of forward and backward traveling waves in region II (material), and

a transmitted wave in region III (air). Imposing the boundary conditions for the electric and magnetic fields at the slab-air interfaces, the transmission coefficient can be calculated in a straightforward manner. The result is

$$T = \frac{E_t e^{-j\beta_0 d}}{E_i} = \frac{4}{e^{\gamma d} \left(2 + \frac{\eta_1}{\eta_2} + \frac{\eta_2}{\eta_1} \right) + e^{-\gamma d} \left(2 - \frac{\eta_1}{\eta_2} - \frac{\eta_2}{\eta_1} \right)} \quad (2)$$

where $\beta_0 = \omega \sqrt{\mu_0 \varepsilon_0} = ((2\pi)/(\lambda)) = ((2\pi f)/(c))$, $\gamma = \alpha + j\beta = j\omega \sqrt{\mu_0 \varepsilon_0 (\varepsilon_r' - j\varepsilon_r'')}$, $\eta_1 = \sqrt{(\mu_0/\varepsilon_0)} = 120\pi\Omega$, and $\eta_2 = \sqrt{((\mu_0)/(\varepsilon_0(\varepsilon_r' - j\varepsilon_r''))})$. The insertion transfer function is related to the transmission coefficient through $T e^{j\beta_0 d} = H(j\omega)$. Thus,

$$H(j\omega) = \frac{4e^{j\beta_0 d}}{e^{\gamma d} \left(2 + \frac{\eta_1}{\eta_2} + \frac{\eta_2}{\eta_1} \right) + e^{-\gamma d} \left(2 - \frac{\eta_1}{\eta_2} - \frac{\eta_2}{\eta_1} \right)} \quad (3)$$

It should be noted that the transmission coefficient T is equivalent to S_{21} in the scattering parameters' terminology.

Once the complex insertion transfer function $H(j\omega)$ is determined by measurements, (3) can be solved for the complex dielectric constant $\varepsilon_r = \varepsilon_r' - j\varepsilon_r''$. In terms of the scattering parameter S_{21} , a parameter that can be directly measured, (3) can be easily cast into the following form [8]:

$$\left(x + \frac{1}{x} \right) \sinh(xP) + 2 \cosh(xP) - \frac{2}{S_{21}} = 0 \quad (4)$$

where $x = \sqrt{\varepsilon_r}$, $S_{21}(j\omega) = H(j\omega)e^{-j\omega\tau_0}$, $P = j\beta_0 d$, and $\tau_0 = d/c$, with d being the layer thickness and c is the speed of light in free space. This equation can be solved numerically using two-dimensional search algorithms. The convergence of this algorithm is not always guaranteed, taking into account possible multiple solutions and noise in the measurements. In Section IV, using reasonable assumptions, (4) is reduced to a one-dimensional problem involving real equations only.

IV. NEW FORMULATION FOR CHARACTERIZATION OF LOW-LOSS MATERIALS

When the material occupying region II is low loss, $\varepsilon_r''/\varepsilon_r' \ll 1$, and the following approximations can be used:

$$\begin{aligned} \gamma &= \alpha + j\beta \\ &= j\omega \sqrt{\mu_0 \varepsilon_0 (\varepsilon_r' - j\varepsilon_r'')} \\ &\cong j\omega \sqrt{\mu_0 \varepsilon_0} \sqrt{\varepsilon_r'} \left(1 - j \frac{1}{2} \frac{\varepsilon_r''}{\varepsilon_r'} \right) \\ &= j\beta_0 \sqrt{\varepsilon_r'} \left(1 - j \frac{1}{2} \frac{\varepsilon_r''}{\varepsilon_r'} \right) \end{aligned} \quad (5)$$

and

$$\eta_2 = \sqrt{\frac{\mu_0}{\varepsilon_0 (\varepsilon_r' - j\varepsilon_r'')}} \cong \sqrt{\frac{\mu_0}{\varepsilon_0 \varepsilon_r'}} = \frac{\eta_1}{\sqrt{\varepsilon_r'}} \quad (6)$$

Then, $(\eta_1/\eta_2) + (\eta_2/\eta_1) \cong \sqrt{\varepsilon_r'} + (1/\sqrt{\varepsilon_r'}) = ((\varepsilon_r' + 1)/(\sqrt{\varepsilon_r'}))$

and (5) reduces to

$$H(j\omega) = \frac{4e^{j\beta_0 d}}{e^{(\alpha+j\beta)d} \left(2 + \frac{\epsilon'_r + 1}{\sqrt{\epsilon'_r}}\right) + e^{-(\alpha+j\beta)d} \left(2 - \frac{\epsilon'_r + 1}{\sqrt{\epsilon'_r}}\right)}. \quad (7)$$

Rewriting the insertion transfer function in terms of magnitude and phase, we obtain (8), shown at the bottom of this page, and

$$\angle H(j\omega) = \beta_0 d - \phi \quad (9)$$

where

$$\phi = \tan^{-1} \left\{ \frac{\left[\frac{e^{\alpha d} \left(2 + \frac{\epsilon'_r + 1}{\sqrt{\epsilon'_r}}\right) - e^{-\alpha d} \left(2 - \frac{\epsilon'_r + 1}{\sqrt{\epsilon'_r}}\right)}{e^{\alpha d} \left(2 + \frac{\epsilon'_r + 1}{\sqrt{\epsilon'_r}}\right) + e^{-\alpha d} \left(2 - \frac{\epsilon'_r + 1}{\sqrt{\epsilon'_r}}\right)} \right] \cdot \tan(\beta d)}{\right\}. \quad (10)$$

Equation (10) can be written in a more compact form as

$$\phi = \tan^{-1} \left\{ \left[\frac{1 - e^{-2\alpha d} Q}{1 + e^{-2\alpha d} Q} \right] \cdot \tan(\beta d) \right\} \quad (11)$$

where

$$Q = - \left(\frac{\sqrt{\epsilon'_r} - 1}{\sqrt{\epsilon'_r} + 1} \right)^2. \quad (12)$$

For most applications of interest, Q has a small value. For example, for the dielectric constants of 2.0, 4.0, and 8.0, Q is approximately 0.02, 0.1, and 0.3, respectively. We will later use this fact to further simplify the solution. For the time being, no assumption is made about Q . Letting $e^{-2\alpha d} = X$, then

$$|H(j\omega)|^2 = \frac{16\epsilon'_r}{\frac{1}{X}(\sqrt{\epsilon'_r} + 1)^4 + X(\sqrt{\epsilon'_r} - 1)^4 - 2\cos(2\beta d)(\epsilon'_r - 1)^2} \quad (13)$$

or

$$X^2 \left(\sqrt{\epsilon'_r} - 1 \right)^4 - 2 \left[\cos(2\beta d) (\epsilon'_r - 1)^2 + 8 \frac{\epsilon'_r}{|H(j\omega)|^2} \right] X + \left(\sqrt{\epsilon'_r} + 1 \right)^4 = 0$$

which is a quadratic equation in terms of X . Solving this equation for X , we have (14), shown at the bottom of this page. Only the solution with a negative sign in (14) is valid (the proof is given in the Appendix). Substituting for X from (14) in the phase expression (11), we obtain the following equation, which is only in terms of ϵ'_r :

$$\tan[\beta_0 d - \angle H(j\omega)] + \frac{1 - QX}{1 + QX} \tan(\beta d) = 0. \quad (15)$$

Solving this equation numerically, ϵ'_r is readily determined. X and subsequently α are then found from (14). Finally, ϵ''_r is calculated using

$$\epsilon''_r = \frac{2c\alpha\sqrt{\epsilon'_r}}{\omega}. \quad (16)$$

The fact that the complex equation (4) can be reduced to a one-dimensional real equation for low-loss materials is illustrated in Fig. 2. This figure shows the magnitude of the left-hand-side expression in (4). As noted, all vertical cuts (parallel to the ϵ'_r -axis) of the surface in Fig. 2 have nearly the same minima points. For better visualization, a vertical cut at $\epsilon''_r = 0.14$ is also shown.

A. Special Case

If it can be further assumed that $e^{-2\alpha d} \ll 1$, then

$$\phi \approx \tan^{-1}(\tan(\beta d)) = \beta d$$

and

$$\angle H(j\omega) = \beta_0 d - \beta d = \beta_0 d - \beta_0 d \sqrt{\epsilon'_r}, \quad \text{where } \beta \approx \beta_0 \sqrt{\epsilon'_r}$$

and

$$\epsilon'_r = \left(1 - \frac{\angle H(j\omega)}{\beta_0 d} \right)^2. \quad (17)$$

Once ϵ'_r is determined, α and then ϵ''_r can be found from

$$|H(j\omega)| = \left(\frac{16}{e^{2\alpha d} \left(2 + \frac{\epsilon'_r + 1}{\sqrt{\epsilon'_r}}\right)^2 + e^{-2\alpha d} \left(2 - \frac{\epsilon'_r + 1}{\sqrt{\epsilon'_r}}\right)^2 + 2\cos(2\beta d) \left(4 - \left(\frac{\epsilon'_r + 1}{\sqrt{\epsilon'_r}}\right)^2\right)} \right)^{(1/2)} \quad (8)$$

$$X = e^{-2\alpha d} = \frac{\left[\cos(2\beta d) (\epsilon'_r - 1)^2 + 8 \frac{\epsilon'_r}{|H(j\omega)|^2} \right] \pm \sqrt{\left[\cos(2\beta d) (\epsilon'_r - 1)^2 + 8 \frac{\epsilon'_r}{|H(j\omega)|^2} \right]^2 - (\epsilon'_r - 1)^4}}{(\sqrt{\epsilon'_r} - 1)^4} \quad (14)$$

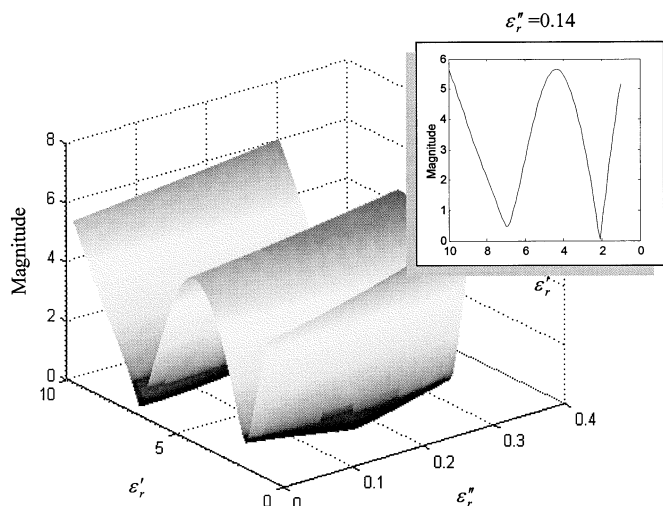


Fig. 2. To illustrate that complex equation (4) can be reduced to a real equation in terms of ϵ'_r for low-loss materials.

$|H(j\omega)|^2$ using the following relationships:

$$|H(j\omega)|^2 \approx \frac{16}{e^{2\alpha d} \left(2 + \frac{\epsilon'_r + 1}{\sqrt{\epsilon'_r}}\right)^2 + 2 \cos(2\beta d) \left[4 - \left(\frac{\epsilon'_r + 1}{\sqrt{\epsilon'_r}}\right)^2\right]} \quad (18)$$

$$\alpha = \frac{1}{2d} \ln \left\{ \frac{16}{|H(j\omega)|^2} + 2 \cos(\beta d) \frac{(\epsilon'_r - 1)^2}{\epsilon'_r} \right\} \cdot \frac{(\sqrt{\epsilon'_r} + 1)^4}{\epsilon'_r} \quad (19)$$

This simplified analysis reduces to the single-pass case, as in [5], where the slab is assumed to be thick, and a single transmitted pulse can be time gated. This is because the assumption $e^{-2\alpha d} \ll 1$ has the implication that the multiple-pass components of the received signal are very small; as for $\alpha d \gg 1$, these components are attenuated significantly more than the single-pass signal.

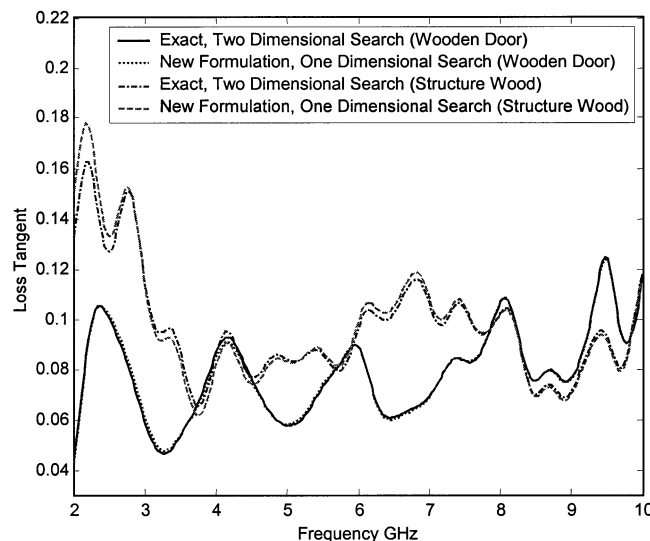
V. MEASUREMENT RESULTS

Measurements were carried out for two sample materials, i.e., a wooden door and structure wood slab. Two wide-band TEM horn antennas were used as a transmitter and receiver. Measurement were performed in both time domain using less than 100-ps pulses and a sampling oscilloscope, and in the frequency domain over a frequency range of 1–12 GHz using a vector network analyzer. The thickness of the sample door is 4.448 cm, while that of the structure wood slab is 2.068 cm. The distance between the two antennas is approximately 3 m, and the sample is placed halfway between the transmitter and receiver. For both samples, the time- and frequency-domain results for the insertion transfer function were essentially the same.

The results for the dielectric constant and the loss tangent obtained from the complex equation (4) and the real equations



(a)



(b)

Fig. 3. Comparison of exact and approximate results for: (a) dielectric constant and (b) loss tangent for two sample materials.

(15) and (16) are compared in Fig. 3(a) and (b). It is noted that the results from the two solutions are nearly identical, primarily because wood is a low-loss material. Both the exact complex and approximate real equations have spurious solutions that can be avoided by starting with an initial guess obtained from the single-pass solution at a high frequency and by using a constrained search. The solution obtained at a high frequency point is then used as an initial guess for the next frequency point because variations of the dielectric constant versus frequency are slow over a narrow frequency range.

In order to assess the accuracy of the approximate method presented above, we take a data point from the measured insertion transfer function $H(j\omega)$ for the sample wooden door at a frequency of 5.00 GHz and artificially increase the loss by decreasing the magnitude of $H(j\omega)$. This is achieved by multiplying $H(j\omega)$ by a constant a , as given in the first row of Table I. A zero-loss case is also included in the table by choosing a such that $a|H(j\omega)| = 1$. As noted, the errors are less than 1% for loss

TABLE I
 ERRORS IN DIELECTRIC CONSTANT AND LOSS TANGENT OBTAINED FROM THE APPROXIMATE FORMULATION.
 (THE DATA POINT USED IN THIS ANALYSIS IS $H(j, u) = -0.3317 - j0.7418$)

		a	1.23	1.0	0.9	0.8	0.7	0.6	0.5	0.4	0.3	0.2	0.1
Exact	ϵ'_r		2.178	2.176	2.174	2.171	2.166	2.159	2.147	2.128	2.095	2.033	1.885
	$\tan \delta$		0	0.063	0.096	0.133	0.176	0.226	0.286	0.363	0.466	0.624	0.940
Approx.	ϵ'_r		2.178	2.176	2.176	2.175	2.175	2.174	2.174	2.174	2.173	2.173	2.173
	%Error		0	0.036	0.972	0.2104	0.406	0.730	1.265	2.162	3.747	6.895	15.312
	$\tan \delta$		0	0.063	0.095	0.132	0.174	0.223	0.281	0.352	0.445	0.575	0.799
	% Error		0	-0.438	-0.485	-0.609	-0.845	-1.243	-1.883	-2.914	-4.631	-7.772	-15.02

tangents of approximately 0.2, a representative upper limit loss factor for most dielectric materials of practical interest. Only for very high-loss cases ($\tan \delta > 0.9$) do the errors become significant, which is approximately 15% for this example. As expected, for the zero-loss case (in this example, corresponding to $a = 1.23$), the approximate solution for the dielectric constant becomes exact. Although this error analysis is for a specific example, it provides a realistic measure of the accuracy of the approximate method presented here.

VI. CONCLUSION

A new formulation for the characterization of low-loss materials has been presented, which requires solving real equations only. This formulation converges more rapidly and, thus, requires much less computation time than that based on solving the complex equation relating the insertion transfer function to the dielectric constant of the material under test. The new formulation can be used to accurately characterize many materials of practical applications. For materials with loss tangents less than 0.2, the results are within 1% error of their respective values obtained from the exact solution.

APPENDIX

Here, it is proven that (14) with a negative sign in front of the square root is the only valid solution. Whenever a solution exists, we must have

$$\left[\cos(2\beta d) (\epsilon'_r - 1)^2 + \frac{8\epsilon'_r}{|H(j\omega)|^2} \right]^2 - (\epsilon'_r - 1)^4 > 0. \quad (\text{A1})$$

Equation (A1) is rewritten as

$$\left[\cos(2\beta d) (\epsilon'_r - 1)^2 + \frac{8\epsilon'_r}{|H(j\omega)|^2} - (\epsilon'_r - 1)^2 \right] \cdot \left[\cos(2\beta d) (\epsilon'_r - 1)^2 + \frac{8\epsilon'_r}{|H(j\omega)|^2} + (\epsilon'_r - 1)^2 \right] > 0. \quad (\text{A2})$$

The second square bracket in (A2) is always positive because

$$\left[\cos(2\beta d) (\epsilon'_r - 1)^2 + \frac{8\epsilon'_r}{|H(j\omega)|^2} + (\epsilon'_r - 1)^2 \right] = \left[(\epsilon'_r - 1)^2 (1 + \cos(2\beta d)) + \frac{8\epsilon'_r}{|H(j\omega)|^2} \right] > 0. \quad (\text{A3})$$

Thus, the first square bracket should also be positive, i.e.,

$$\cos(2\beta d) (\epsilon'_r - 1)^2 + \frac{8\epsilon'_r}{|H(j\omega)|^2} - (\epsilon'_r - 1)^2 > 0$$

or

$$\cos(2\beta d) (\epsilon'_r - 1)^2 + \frac{8\epsilon'_r}{|H(j\omega)|^2} > (\epsilon'_r - 1)^2 > 0. \quad (\text{A4})$$

Hence, the solution for X with a negative sign in front of the square root is always > 0 , i.e., (A5), shown at the bottom of this page. On the other hand, X should be less than one (otherwise, instead of attenuation, we have amplification). It can be easily verified that the solution for X with a positive sign in front of the square root is greater than one and, thus, is not acceptable. The correct solution is the one with the minus sign in front of the square root.

$$X = \frac{\left[\cos(2\beta d) (\epsilon'_r - 1)^2 + 8 \frac{\epsilon'_r}{|H(j\omega)|^2} \right] - \sqrt{\left[\cos(2\beta d) (\epsilon'_r - 1)^2 + 8 \frac{\epsilon'_r}{|H(j\omega)|^2} \right]^2 - (\epsilon'_r - 1)^4}}{(\sqrt{\epsilon'_r} - 1)^4} \quad (\text{A5})$$

REFERENCES

- [1] T. Gibson and D. Jenn, "Prediction and measurements of wall insertion loss," *IEEE Trans. Antennas Propagat.*, vol. 47, pp. 55–57, Jan. 1999.
- [2] I. Cuinas and M. Sanchez, "Building material characterization from complex transmissivity measurements at 5.8 GHz," *IEEE Trans. Antennas Propagat.*, vol. 48, pp. 1269–1271, Aug. 2000.
- [3] J. Zhang, M. Nakhsh, and Y. Huang, "In-situ characterization of building materials," in *11th Int. Antennas and Propagation Conf.*, Apr. 17–20, 2001, Conf. Pub. 480, pp. 269–274.
- [4] J. Baker-Jarvis, R. G. Geyer, J. H. Grosvenor, Jr., M. D. Janecic, C. A. Jones, B. Riddle, C. M. Weil, and J. Krupka, "Dielectric characterization of low-loss materials: A comparison of techniques," *IEEE Trans. Dielect. Elect. Insulation*, vol. 5, pp. 571–577, Aug. 1998.
- [5] F. J. Aurand, "Measurements of transient electromagnetic propagation through concrete and sand," Sandia Nat. Labs., Livermore, CA, Sandia Rep. SAND96-2254 UC-706, Sept. 1996.
- [6] J. Baker-Jarvis, E. J. Vanzura, and W. A. Kissck, "Improved technique for determining complex permittivity with the transmission/reflection method," *IEEE Trans. Microwave Theory Tech.*, vol. 38, pp. 1096–1103, Aug. 1990.
- [7] D. Kralj and L. Carin, "Ultra-wideband characterization of lossy materials: Short-pulse microwave measurements," in *IEEE MTT-S Int. Microwave Symp. Dig.*, vol. 13, 1993, pp. 1239–1242.
- [8] W. Su, R. Mostafa, S. M. Riad, and I. L. Al-Qadi, "Characterization of concrete material using TEM horn antennas," in *URSI Nat. Radio Science Meeting Dig.*, Boulder, CO, Jan. 1996, p. 140.

Ali Hussein Muqaibel (S'95) received the B.Sc. and M.Sc. degrees in electrical engineering from the King Fahd University of Petroleum and Minerals (KFUPM), Dhahran, Saudi Arabia, in 1996 and 1999, respectively, and is currently working toward the Ph.D. degree at the Virginia Polytechnic Institute and State University, Blacksburg.

From 1996 to 1999, he was an Electrical Engineer with KFUPM. He was later a Lecturer with KFUPM for one year until 2000. He is currently with the Time Domain and RF Measurements Laboratory, Mobile and Portable Radio Research Group, Virginia Polytechnic Institute and State University. He has coauthored over 20 journal and conference publications. His main area of interest includes measurements for channel characterization and ultra-wide-band communications.

Ahmad Safaai-Jazi (S'77–M'78–SM'86) received the B.Sc. degree from the Sharif University of Technology, Tehran, Iran, in 1971, the M.A.Sc. degree from the University of British Columbia, Vancouver, BC, Canada, in 1974, and the Ph.D. degree (with distinction) from McGill University, Montreal, QC, Canada, in 1978, all in electrical engineering.

From 1978 to 1984, he was an Assistant Professor with the Division of Electrical and Computer Engineering, Isfahan University of Technology. From 1984 to 1986, he was a Research Associate with the Department of Electrical Engineering, McGill University. He then joined the Virginia Polytechnic Institute and State University, Blacksburg, where he is currently a Professor with the Bradley Department of Electrical and Computer Engineering. At the Virginia Polytechnic Institute and State University, he has introduced and developed the new graduate course, "Optical Waveguides—Theory and Applications," which is a principal graduate course in the fiber-optic program. He has authored or coauthored over 100 refereed journal papers and conference publications. He has contributed one book chapter and holds three patents. His research interests include guided-wave optics, antennas and propagation, wide-band characterization of dielectric materials, and ultra-wide-band communications.

Dr. Safaai-Jazi is a member of the Optical Society of America. He was the corecipient of the 1995 Wheeler Award for the best application paper presented by the IEEE Antennas and Propagation Society (IEEE AP-S). He was a recent recipient of the Dean's Award for Excellence in Teaching presented by the College of Engineering at the Virginia Polytechnic Institute and State University.